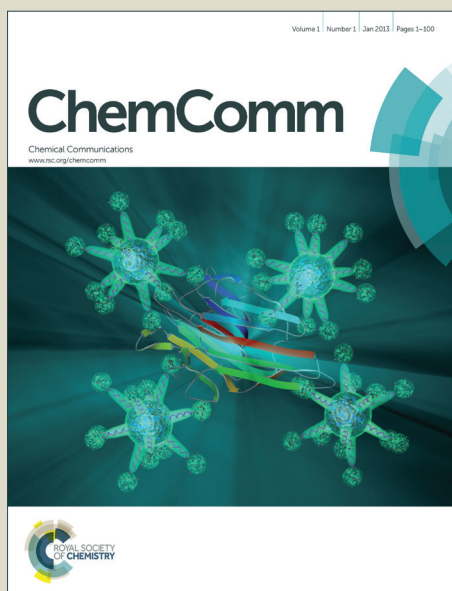This is an *Accepted Manuscript*, which has been through the Royal Society of Chemistry peer review process and has been accepted for publication.

Accepted Manuscripts are published online shortly after acceptance, before technical editing, formatting and proof reading. Using this free service, authors can make their results available to the community, in citable form, before we publish the edited article. We will replace this *Accepted Manuscript* with the edited and formatted *Advance Article* as soon as it is available.

You can find more information about *Accepted Manuscripts* in the **Information for Authors**.

Please note that technical editing may introduce minor changes to the text and/or graphics, which may alter content. The journal's standard **Terms & Conditions** and the **Ethical guidelines** still apply. In no event shall the Royal Society of Chemistry be held responsible for any errors or omissions in this *Accepted Manuscript* or any consequences arising from the use of any information it contains.

Journal Name

COMMUNICATION

Hexaphenylbenzene Based AIEE Active Two Photon Probe for Detection of Hydrogen Sulfide with Tunable Self-assembly in Aqueous Media and Application in Live cell Imaging

Subhamay Pramanik,[a] Vandana Bhalla*,[a] Hwan Myung Kim,[b] Hardev Singh [b], Hyo Won Lee[b] and Manoj Kumar*[a]

Supramolecular aggregates of hexaphenylbenzene derivative 2 exhibit aggregation induced emission enhancement and modulation of self-assembled architecture from spherical to flower like assembly in presence of H_2S. Furthermore, the probe 2 displays higher photostability, low toxicity and bright green fluorescence in two-photon microscopy (TPM) imaging for the detection of H_2S in live HeLa cells.

Hydrogen sulfide (H_2S), a newly recognized neurotransmitter,[1a] is generated in mammalian tissues from cysteine and homocysteine through the action of various enzymes such as cystathionine β-synthase (CBS) and cystathionine γ-lyase (CSE).[1b] The involvement of H_2S has been validated in various physiological processes,[1c] such as regulation of cell growth, cardiovascular protection, modulation of neuronal transmission and anti-inflammation effect.[1d] However, any imbalance in H_2S level leads to a variety of diseases such as Parkinson's disease (PD)[1e] Alzheimer's[2a] disease and Down's syndrome,[2b] diabetes,[2c] and liver cirrhosis. Thus, to check this imbalance, monitoring of H_2S in live cells and tissues is crucial. In this context, a variety of fluorescent probes have been developed for trace detection of H_2S, however, most of these probes are based on one-photon dyes.[3] The one photon excitation microscopy based probes for bioimaging require a rather short excitation wavelength (usually UV-vis photon 350-500 nm) which limits their biological applications because of the photobleaching phenomenon, cell damage, auto fluorescence by exciting natural fluorophores such as nicotinamide adenine dinucleotide and flavin adenine dinucleotide. On the other hand, probes based on two-photon microscopy (TPM) offer a number of advantages, including greater penetration depth (>500 μm), longer excitation wavelength, and longer observation time.[4] Though there are several reports on two photon-excited (TPE)

probes[4] for the detection of H_2S, yet, most of them suffer from limitations such as slow response time, single wavelength centred emission, poor detection limit and interference from other biologically relevant species.[5] Therefore, development of rapid, highly sensitive and selective two photon active probe for the detection of H_2S in solution and in live cells has been a formidable challenge yet to be achieved.
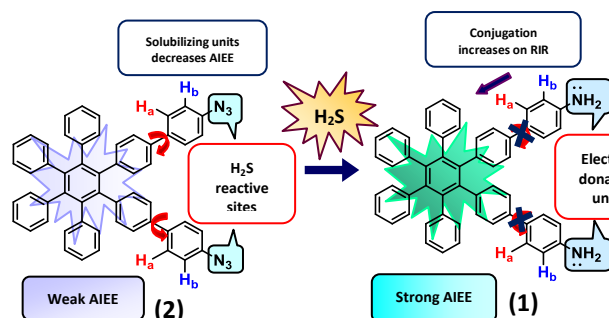
Scheme 1. Designing strategy for monitoring H_2S and H_2S induced AIEE.

Keeping this in view, we envisaged that if we could design a two photon active probe with an effective H_2S reaction center which in the presence of H_2S gives a product that can undergo aggregation induced emission enhancement then it will be possible to overcome the above mentioned limitations and thus, for this purpose we designed and synthesized hexaphenylbenzene (HPB) based probe 2 having azide groups as H_2S reaction centres (Scheme 1). HPB is scaffold of our choice due to its AIEE characteristics[6] and two photon cross section area[5e]. Interestingly, derivative 2 can diffuse through cell membrane due to its higher solubility and in presence of H_2S it undergoes reduction to furnish derivative 1 which has aggregation induced emission (AIEE) characteristics to show bright fluorescence. The designed probe 2 has many advantages: (i) supramolecular assemblies of HPB derivative 2 served as 'not quenched' AIEE active probe for selective detection of H_2S in aqueous media and in vapour phase. Recently, Tang et. al., reported a tetraphenylethene-based AIE active probe for the detection of H_2S only in solution phase,[7] and, the emission changes were centred around single wavelength. In comparison, the supramolecular aggregates of derivative 2 exhibit emission changes at two distinct wavelengths as the fluorescent sensors showing response at two

[a] Department of Chemistry, UGC Sponsored Centre for Advanced Studies-1, Guru Nanak Dev University, Amritsar 143005, and Punjab, India Fax: +91 (0)183 2258820; Tel: +91 (0)183 2258802-9 ext.3202, 3205.
E-mail: vanmanan@yahoo.co.in, mksharmaa@yahoo.co.in
[b] Department of Chemistry and Department of Energy Systems Research, Ajou University, Suwon 443-749, Korea. E-mail: kimhm@ajou.ac.kr
† Electronic Supplementary Information (ESI) available. For ESI please see DOI: 10.1039/x0xx00000x

different wavelengths are more advantageous due to less interference from fluctuations of background fluorescence. (ii) TPE probe **2** can detect H_2S upto 0.33 µM level, which is one of the best among the reported probes. (iii) Furthermore, for the first time, the sensing event was accompanied by H_2S mediated morphology change of probe from spherical to flower like self-assembled architecture. (iv) The high photostability, low toxicity, strong emission enhancement ($\geq$30 folds enhancement) and high TP action cross section area of derivative **2** in the presence of H_2S makes it a useful tool for the detection of H_2S in live HeLa cells at higher penetration depth. To the best of our knowledge, this is the first report where the two photon excited AIEE active HPB based supramolecular assemblies have been utilized for the detection of H_2S in live HeLa cells with minimal interference (Table S1, ESI†).

The synthesis of the probe **2** is given in scheme S1 (ESI†). The structure of compound **2** was confirmed from its spectroscopic and analytical data (Fig. S29-S32, ESI†). The molecular recognition behaviour of probe **2** towards H_2S was studied by the UV-vis and fluorescence studies in H_2O/DMSO (7:3, v/v) mixture. The UV-vis spectrum of derivative **2** in DMSO exhibits an absorption band at 300 nm due to π-π* transition. On addition of 400 µM Na_2S solution in HEPES buffer to the solution of **2**, an increase in intensity of absorption band at 300 nm was observed along with the appearance of a level-off tail in the visible region (Fig. S1A-B, ESI†).
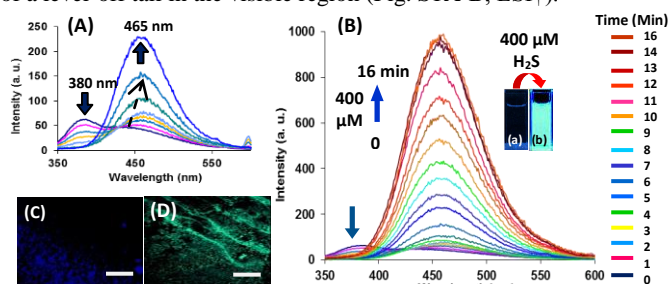
Fig. 1 (A) Showing the variation in fluorescence intensity of probe **2** at two different wavelength 380 and 465 nm within first 6 min after H_2S addition; (B) Time dependent fluorescence spectra of **2** (5 µM), after incubation with 400 µM H_2S in H_2O/DMSO (7:3, v/v) mixtures, buffered with HEPES (pH = 7.05) mixtures, λ_{ex} = 300 nm; inset showing the change in fluorescence (a) before and (b) after the addition of 400 µM H_2S under 365 nm UV light; Confocal images showing the change in fluorescence intensity of supramolecular aggregates of **2** (C) before and (D) after the addition of H_2S, λ_{ex} = 405 nm; Scale bar 10 µm.

The solution of derivative **2** in H_2O/DMSO (7:3, v/v) is weakly emissive and exhibits an emission maxima at 380 nm with a broad band at 450 nm on excitation at 300 nm (Fig. 1A). Upon addition of 50 µM (10 equiv.) buffered solution of Na_2S to the solution of **2**, decrease in emission intensity of the band at 380 nm is observed along with gradual red-shift of the broad band from 450 to 465 nm within first 6 min (Fig. 1A). Upon further addition of 70 equiv. of Na_2S solution (350 µM) in HEPES, $\geq$30 folds enhancement in emission intensity of the band at 465 nm was observed (Φ = 0.65) in 10 min (Fig. 1B). The enhancement in fluorescence intensity is observed at 465 nm with the addition of increasing concentrations of Na_2S solution (upto 400 µM) to the solution of probe **2** (Fig. S2A, ESI†). The graph plotted between emission intensity at 465 nm *vs* the conc. of Na_2S added is almost linear when concentration of Na_2S is below 100 µM (Fig. S2B, ESI†). These studies clearly demonstrate that the detection of H_2S by the aggregates of **2** has a threshold concentration, below which small fluorescence enhancement is observed, and above this threshold value (100 µM) a

sharp increase in emission intensity is observed. The fluorescence quenching at 380 nm may be attributed to the reduction of probe **2** and the enhancement in the emission intensity at 465 nm is attributed to the aggregation induced emission enhancement characteristic of the reduced product **1** (Scheme S2, ESI†).[7] These spectral changes clearly indicate that derivative **2** served as 'not quenched' active probe for selective detection of H_2S in aqueous media.
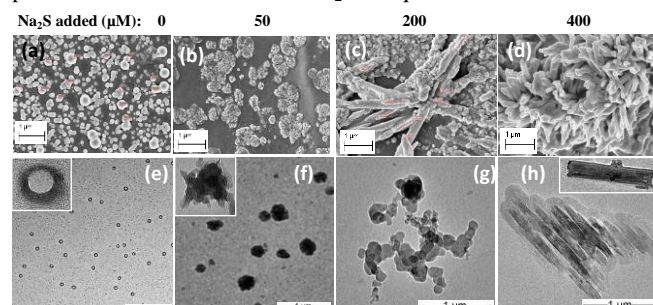
Fig. 2 SEM (a-d) and TEM (e-h) images showing (a & e) spherical aggregates of derivative **2** in H_2O/DMSO (7:3, v/v); After addition of H_2S at various concentration: (b & f) after 50 µM Na_2S addition self-assembled spherical microspheres, (c & g) after 200 µM Na_2S addition rods or chain by self-assembled microspheres and (d & h) self-assembly of micro-rod after the addition of 400 µM Na_2S in the solution of **2** in H_2O/DMSO (7:3, v/v), suggest the formation of more packed supramolecular aggregates.

The progress of the reduction process was also studied by the time-resolved fluorescence spectroscopy (TRF) (Fig. S3, ESI†). The fluorescence life time decay of derivative **2** in H_2O/DMSO (7:3, v/v) buffered with HEPES, pH = 7.05 was obtained by fitting the time resolved curves based on bi-exponential function at 465 nm. In the absence of H_2S, the half-life of excited state I (τ_1) and II (τ_2) was in the order of 0.72 and 2.54 ns, where major fractions of molecules (90%) undergo radiative decay through the fast pathway (τ_1 = 0.72 ns). This result suggests that major fraction of the molecules are present in non-aggregated form. Further, after the addition of H_2S, both the life time τ_1 and τ_2 increased to 1.03 and 5.34 ns; major fractions (80%) of the molecules were found to decay through the slower pathway (τ_2 = 5.34 ns). This result indicates the formation of ordered aggregates. A very small difference between fluorescence radiative rate constants (k_f) of derivative **2** before (0.081×10^9 s^{-1}) and after (0.13×10^9 s^{-1}) the addition of H_2S was observed; however, large decrease in case of non-radiative decay constant (k_{nr}) was observed from 0.86×10^9 s^{-1} to 0.07×10^9 s^{-1} in the presence of H_2S (Table S2, ESI†). These studies suggest that the restriction in the intramolecular rotation of the rotors linked to the core is the main reason of the AIEE phenomena in case of reduction of derivative **2** in presence of H_2S. We believe that presence of azido groups at the periphery of the aggregates increases the solubility of derivative **2** in mixed aqueous media and most of the molecules are present in non-aggregated form. However, in the presence of H_2S, azido groups are reduced to amino groups which decreases the solubility of the molecules in aqueous media hence, major fraction of the molecules are present in the aggregated form leading to the emission enhancement. The time resolved fluorescence studies support these assumptions (*vide supra*). The formation of the aggregates restricts the rotations of the molecules, induces planarization and makes the molecules more rigid and emissive. The confocal microscopy image of compound **2** in H_2O/DMSO (7:3, v/v) clearly indicates the presence of blue luminescent aggregates whereas in presence of H_2S bright green luminescent architecture was observed (Fig. 1C-D). Further, the

Journal Name

COMMUNICATION

scanning electron microscopic (SEM) and transmission electron microscopic (TEM) images showed that derivative **2** in H_2O/DMSO (7:3, v/v) formed spherical aggregates (Fig. 2a and e), whereas on addition of increasing concentrations of Na_2S solution from 50, 200 to 400 μM, self-assembled spherical aggregates (Fig. 2b and f), rod or chain like assembly (Fig. 2c and g) and packed flower shaped micro-rods (Fig. 2d and h) were observed, respectively (Fig. S4 & Scheme S3, ESI†). Dynamic light scattering studies also indicate that size of the aggregates varies from 350 to 1500 nm on addition of 400 μM Na_2S (Fig. S5, ESI†). These studies suggest the change in morphology and size of the aggregates in presence of H_2S. On the basis of fluorescence, TRF, SEM, TEM and DLS studies, we believe that restriction to rotation (RIR) and aggregation driven growth are the main reasons for the fluorescence enhancement. The detection limit of aggregates of **2** for H_2S was found to be 0.33 μM (Fig. S6, Table S3, ESI†). A good corelation was observed between exact concentration of H_2S and experimental values obtained by using derivative **2**, thus, it can be utilized as quantitative probe for the detection of H_2S at micromolar level.

To get insight into the mechanism, we have carried out a reaction of derivative **2** (1 M) with H_2S (aqueous solution of Na_2S, 2.5 M) and the reduced product was isolated and characterized by ^1H and ^{13}C NMR and ESI-MS studies. These spectroscopic data confirm the formation of compound **1** (Fig. S33-S35, ESI†). The overlay of ^1H NMR spectra shows the appearance of new peak at 3.48 ppm corresponding to protons of amino groups and up-field shift of 0.27 and 0.3 ppm for the H_a and H_b aromatic protons which confirms the conversion of azide group to amino moiety in the presence of H_2S (Fig. S7, ESI†). In the FT-IR spectrum, the appearance of a peak at 3385 cm^{-1} corresponding to amino group and disappearance of peak at 2094 cm^{-1} corresponding to azido group clearly indicates the formation of compound **1** (Fig. S8, ESI†). The rate constant for the formation of **1** from **2** was found to be 2.39×10^{-2} min^{-1} (Fig. S9, ESI†). On addition of water content up to 70% (volume fraction) to the DMSO solution of **2**, no significant change in the UV-vis and fluorescence spectrum was observed (Fig, S10-S11, ESI†) while, in case of reduced product **1**, enhancement in the emission intensity (Φ = 0.66) is observed at 465 nm (Fig. S12, ESI†). The UV-vis spectra showed gradual increase in intensity of entire absorption spectra with the appearance of a level-off tail in the visible region (Fig. S13, ESI†). Further, the fluorescence intensity also increases with increasing viscosity on adding glycerol to DMSO solution and decrease in fluorescence intensity was observed with increasing temperature (Fig. S14-S17, ESI†). Furthermore, the concentration dependent ^1H NMR studies of compound **1** showed an upfield shift of 0.08 ppm in case of protons corresponding to HPB moiety which may be due to the intermolecular π-π stacking between the HPB based molecules (Fig. S18, ESI†). The time resolved fluorescence spectra of **1** also showed the large decrease in case of non-radiative decay constant (k_{nr}) from 1.07×10^9 s^{-1} to 0.067×10^9 s^{-1} which accelerated the deactivation of nonradiative decay due to restriction in intramolecular rotation (RIR) of the rotors (Fig. S19, Table S4, ESI†). The above studies confirm that the AIEE characteristics of derivative **1** is the principal reason for the observed emission enhancement.

In addition to being a health hazard, the unpleasant odour of H_2S detectable in the range of >10 ppb, is considered a public

nuisance. Till date all the reported chemosensors for H_2S were at molecular level only and are suitable for the detection of H_2S only in solution phase, whereas, detection of H_2S in vapour phase is still a challenge. Due to the porous nature of aggregates of derivative **2**, the detection of H_2S in vapour phase is also possible which is unprecedented in literature. Keeping this in mind, we were interested to examine the sensitivity of **2** towards H_2S in vapour phase. For this purpose, we exposed the solution of aggregates of derivative **2** in H_2O/DMSO (7:3, v/v) to the vapours of H_2S. A 8-folds emission enhancement at 465 nm was observed within 60 minutes of exposure to vapours of H_2S at room temperature (Fig. S20A-B, ESI†). These results indicate that aggregates of the **2** exhibit 'not quenched' response to H_2S in solution as well as in vapour phase. To check the selectivity, we also examined the response of supramolecular aggregates of derivative **2** towards H_2S in the presence of vapours of various sulphur containing compounds with unpleasant odour such as thiophene and carbon disulphide (CS_2) and it was found that **2** is selective and sensitive to H_2S only. We also studied the vapour phase detection of H_2S in the presence of common smell evolving chemicals like benzene, toluene, pyridine and ammonia but no interference was observed (Fig. S20C, ESI†).

The practical utility of derivative **2** for the detection of H_2S in solid state was also investigated by preparing compound **2**-coated paper strips by dipping the Whatman filter paper into the solution of **2** followed by drying the strips under vacuum. A solution of Na_2S in buffer (10^{-3} M) was sprayed onto the strip by writing "H_2S", and the solvent was evaporated in air. Bright blue fluorescence appeared on the regions exposed to Na_2S solution (Fig. S21A, ESI†). Bright sky blue fluorescent spots of different intensities were observed with different concentrations of Na_2S in HEPES buffer which shows that the regulation of the stimulating behavior of **2** is practically applicable by varying the concentration of even up to the level of 10^{-7} M (Fig. S21B, ESI†). These results make derivative **2** a powerful tool for the instant detection of H_2S for practical applications.
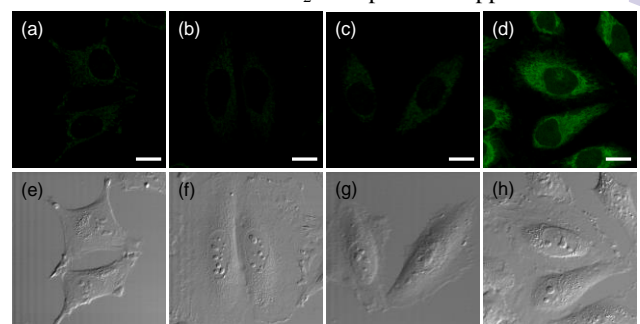

Fig. 3 TPM images of HeLa cells labeled with (a) 20 μM **2** for 30 min. Cells were pretreated with 1 mM (b) GSH, (c) Cysteine, and (d) Na_2S for 30 min before labeling with **2**. (e-h) DIC images. The TPM images were obtained by collecting the TPEF at 400–600 nm upon excitation at 710 nm with femtosecond pulses. Cells shown are representative images from replicate experiments (n = 3). Scale bar: 20 μm.

We also carried out fluorescence studies of derivative **2** with various anions, such as F$^-$, Cl$^-$, Br$^-$, I$^-$, SO_4^{2-}, CO_3^{2-}, NO_3^-, AcO$^-$, $H_2PO_4^-$, ClO$^-$, $S_2O_3^{2-}$ (400 μM for each) as their tetrabutylammonium salts, reactive oxygen species (ROS) such as H_2O_2 and ClO$^-$ (400 μM for each) and biologically relevant species such as cysteine, homocysteine and glutathione biothiols, however, no significant

change in fluorescence behaviour was observed (Fig. S22, ESI†). Derivative **2** displayed strong response upon addition of 400 μM Na_2S in HEPES buffer in the presence of GSH (1 mM) or Cys (1 mM) thereby confirming the high selectivity of **2** towards H_2S over GSH and Cys. We also studied the effect of pH on the recognition behavior of aggregates of **2** towards H_2S which exists in equilibrium with HS^-/S^{2-} at pH 7. It was found that fluorescence enhancement is faster in basic pH than in acidic pH (Fig. S23, ESI†). This faster enhancement in fluorescence emission at pH>7 is due to the existence of H_2S as HS^- under basic conditions which has more reducing power in comparison to H_2S which exists in acidic pH. Further, derivative **2** could detect H_2S in blood serum containing Na_2S and real water samples, including tap water and ground water spiked with the solution of Na_2S (Fig. S24-S25, ESI†). The excellent selectivity of derivative **2** for H_2S over other reactive analytes makes it a promising tool for the detection of H_2S in complex biological environment by taking advantage of AIEE phenomena.
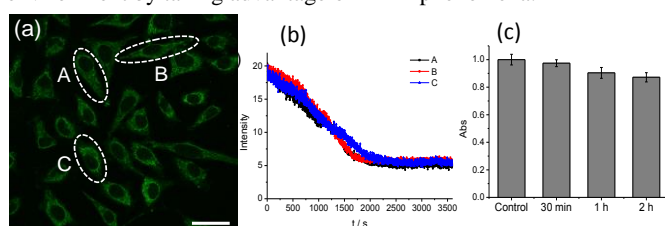

Fig. 4 (a) TPM image of **3**-labeled HeLa cells after treated with Na_2S for 30 min. (b) Relative TPEF intensity from in Figure (a) as a function of time. The digitized intensity was recorded with 2.00 sec intervals for the duration of one hour using *xyt* mode. The TPEF intensities were collected at 400-600 nm upon excitation at 710 nm with femto-second pulses. Cells shown are representative images from replicate experiments (n = 3). Scale bar: 48 μm; (c) Viability of HeLa cells in the presence of **2** as measured by using CCK-8 kit. The cells were incubated with 20 μM **2** for 30 min, 1 hr, and 2 hrs. Six independent experiments are performed.

Keeping in view the fluorescence enhancement (≥30 folds enhancement) of probe **2** in the presence of H_2S in aqueous media with higher sensitivity and selectivity, we were interested in utilization of probe **2** for the detection H_2S in the live HeLa cells. Derivative **2** displayed very low toxicity toward live cells as determined using a CCK-8 kit (Fig. 4c), thus, making it a useful candidate for various biological applications. The TP action cross section area ($\Phi\delta_{max}$, where δ is the TP absorption cross section) were determined by investigating the TPEF spectra with rhodamine 6G as the reference. The $\Phi\delta_{max}$ value for **2** was too small to be determined, however, in the presence of Na_2S TP action cross section area increased significantly to 1.31 GM (1 GM = 10^{-50} cm^4 s photon^{-1}) (Table S5 and Fig. S26-S27, ESI†). Keeping this in mind, we examined the applicability of the aggregates of **2** for the detection of H_2S through TPM imaging in living cells. TPM image of HeLa cells labelled with **2** was very weak (Fig. 3a) but on addition of H_2S it became very bright (Fig. 3d). These results clearly indicate the easy loading, convenient rate of H_2S-induced reduction to form AIEE active product, and high $\Phi\delta_{max}$ value of the reduced product making this a useful tool for the detection of H_2S in live cells at higher penetration depth. In comparison, cells pre-treated with biothiols such as 1 mM GSH, cysteine showed no significant change in emission (Fig. 3b-c). The probe **2** showed good photostability as measured in the HeLa cells at different time intervals (Fig. 4a-b). Therefore, probe **2** possess good cell penetration and has a potential to serve as an efficient AIEE active probe for the study of biological

processes involving H_2S within live cells with negligible interference from other biologically relevant species (Fig. S28, ESI†).

In conclusion, we designed and synthesized hexaphenylbenzene based TPE active probe **2** by coupling aggregation induced emission enhancement (AIEE) phenomena with the reduction based strategy of azido functionality in presence of H_2S. Supramolecular aggregates of derivative **2** exhibit emission enhancements (≥30 folds) and modulation of self-assembled architecture from spherical to closely packed flower like micro-rods in the presence of H_2S. Furthermore, the probe **2** displays high photostability, low toxicity and exhibit bright green fluorescence in live HeLa cells in two-photon microscopy (TPM) imaging in presence of H_2S without interference from other biologically relevant species.

Notes and references

1   (a) C. Zabo, *Nat. Rev. Drug. Discov.*, 2007, **6**, 917; (b) G. D. Yang, L. Wu, B. Jiang, W. Yang, J. Qi, K. Cao, Q. Meng, A. K. Mustafa, W. Mu, S. Zhang, S. H. Snyder and R. Wang, *Science*, 2008, **322**, 587; (c) R. Baskar and J. Bian, *Eur. J. Pharmacol.*, 2011, **656**, 5; (d) C. Yang, Z. Yang, M. Zhang, Q. Dong, X. Wang, A. Lan, F. Zeng, P. Chen, C. Wang and M. Feng, *PLoS One*, 2011, **6**, 21971; (e) L. F. Hu, M. Lu, C. X. Tiong, G. S. Dawe, G. Hu and J. S. Bian, *Aging Cell*, 2010, 135.

2   (a) K. Eto, T. Asada, K. Arima, T. Makifuchi and H. Kimura, *Biochem. Biophys. Res. Commun.*, 2002, **293**, 1485; (b) P. Kamoun, M.-C. Belardinelli, A. Chabli, K. Lallouchi and B. Chadefaux-Vekemans, *Am. J. Med. Genet.*, 2003, **116A**, 310; (c) W. Yang, G. Yang, X. Jia, L. Wu and R. Wang, *J. Physiol.*, 2005, **569**, 519; (d) S. Fiorucci, E. Antonelli, A. Mencarelli, S. Orlandi, B. Renga, G. Rizzo, E. Distrutti, V. Shah and A. Morelli, *Hepatology*, 2005, **42**, 539.

3   (a) C. Zhang, L. Wei, C. Wei, J. Zhang, R. Wang, Z. Xi and L. Yi, *Chem. Commun.*, 2015, **51**, 7505; (b) J. Cao, R. Lopez, J. M. Thacker, J. Y. Moon, C. Jiang, S. N. S. Morris, J. R. Bauer, P. Tao, R. P. Mason and A. R. Lippert, *Chem. Sci.*, 2015, **6**, 1979; (c) L. Yuan, F. Jin, Z. Zeng, C. Liu, S. Luo and J. Wu, *Chem. Sci.*, 2015, **6**, 2360; (d) N. Gupta, S. I. Reja, V. Bhalla, M. Gupta, G. Kaur and M. Kumar, *Chem. Commun.*, 2015, **51**, 10875.

4   (a) S. K. Bae, C. H. Heo, D. J. Choi, D. Sen, E.-H. Joe, B. R. Cho, and H. M. Kim, *J. Am. Chem. Soc.*, 2013, **135**, 9915; (b) H. M. Kim and B. R. Cho, *Chem. Commun.*, 2009, 153; (c) W. Sun, J. Fan, C. Hu, J. Cao, H. Zhang, X. Xiong, J. Wang, S. Cui, S. Sun and X. Peng, *Chem. Commun.*, 2013, **49**, 3890; (d) C. S. Lim, S. K. Das, S. Y. Yang, E. S. Kim, H. J. Chun and B. R. Cho, *Anal. Chem.*, 2013, **85**, 9288.

5   (a) C. S. Lim, G. Masanta, H. J. Kim, J. H. Han, H. M. Kim and B. R. Cho, *J. Am. Chem. Soc.*, 2011, **133**, 11132; (c) H. M. Kim and B. R. Cho, *Acc. Chem. Res.*, 2009, **42**, 863; (d) A. R. Sarkar, C. H. Heo, E. Kim, H. W. Lee, H. Singh, J. J. Kim, H. Kang, C. Kang and H. M. Kim, *Chem. Commun.*, 2015, **51**, 2407; (e) S. Yao and K. D. Belfield, *Eur. J. Org. Chem.*, 2012, 3199.

6   (a) Y. Hong, J. W. Y. Lam and B. Z. Tang, *Chem. Soc. Rev.*, 2011, **40**, 5361; (b) S. Pramanik, V. Bhalla, and M. Kumar, *ACS Appl. Mater. Interfaces*, 2014, **6**, 5930; (c) V. Bhalla, S. Pramanik and M. Kumar, *Chem. Commun.*, 2013, **49**, 895.

7   Y. Cai, L. Li, Z. Wang, J. Z. Sun, A. Qin and B. Z. Tang, *Chem. Commun.*, 2014, **50**, 8892.